A method of recovering the initial vectors of globally coupled map lattices based on symbolic dynamics*

Sun Li-Sha(孙丽莎)[a)†], Kang Xiao-Yun(康晓云)[a)], Zhang Qiong(张 琼)[b)], and Lin Lan-Xin(林兰馨)[c)]

[a)] *College of Engineering, Shantou University, Shantou* 515063, *China*

[b)] *Department of Science and Technology, University of Science and Technology of China, Hefei* 230026, *China*

[c)] *Department of Electronic Engineering, City University of Hong Kong, Hong Kong, China*

(Received 29 December 2010; revised manuscript received 23 June 2011)

Based on symbolic dynamics, a novel computationally efficient algorithm is proposed to estimate the unknown initial vectors of globally coupled map lattices (CMLs). It is proved that not all inverse chaotic mapping functions are satisfied for contraction mapping. It is found that the values in phase space do not always converge on their initial values with respect to sufficient backward iteration of the symbolic vectors in terms of global convergence or divergence (CD). Both CD property and the coupling strength are directly related to the mapping function of the existing CML. Furthermore, the CD properties of Logistic, Bernoulli, and Tent chaotic mapping functions are investigated and compared. Various simulation results and the performances of the initial vector estimation with different signal-to-noise ratios (SNRs) are also provided to confirm the proposed algorithm. Finally, based on the spatiotemporal chaotic characteristics of the CML, the conditions of estimating the initial vectors using symbolic dynamics are discussed. The presented method provides both theoretical and experimental results for better understanding and characterizing the behaviours of spatiotemporal chaotic systems.

Keywords: coupled map lattices, symbolic dynamics, initial condition estimation, convergence or divergence property

PACS: 05.45.Xt, 05.45.–a, 07.05.Kf **DOI:** 10.1088/1674-1056/20/12/120507

1. Introduction

Chaos is the most common phenomenon in a nonlinear system, and has been widely studied. However, in the practical applications of various nonlinear systems there exist spatiotemporal chaotic characteristics.[1−3] The behaviour of the spatiotemporal chaotic system can be affected by any small turbulence of the initial state. The coupled map lattice (CML) model is an important model for describing spatiotemporal chaotic behaviour, and which describes a dynamic system with discrete time and space dimensions and continuous state variables. CML provides the dynamics of the local discrete time of the lattices and the spatial coupling between the lattices.[4,5] The types of spatial coupling indicate the different interactions between the multichannel signals in space of the CML model. The general method of describing the CML includes both global coupling and local coupling, which provides various mathematical models which describe different practical spatiotemporal chaotic systems.[6−8]

The CML model provides a useful way of analysing spatiotemporal chaotic phenomena. Based on symbolic dynamics, a computationally efficient algorithm can be obtained to describe the spatiotemporal chaotic model. Symbolic dynamics is regarded as a coarse-grained description of trajectories for various systems. It is robust and the statistical characteristics of the system invariant can be kept by symbolic vectors, which provide an effective way of describing the orbits of the nonlinear dynamical system. For example, symbolic entropy in terms of symbolic dynamics has been introduced to quantitatively compute the information about the existing chaotic sequences.[9,10] The dynamic symbolic vector is also employed to determine the pseudo-randomness of the nonlinear chaotic system and the ergodicity of CML.[11,12]

The symbolic dynamics of the global CML model is introduced by Shawn *et al.*,[13] but the issue of estimating the initial vectors of the global CML has not

*Project supported by the National Natural Science Foundation of China (Grant Nos. 61072037 and 60271023) and the Natural Science Foundation of Guangdong Province, China (Grant No. 10151503101000011).

†Corresponding author. E-mail: lssun@stu.edu.cn

© 2011 Chinese Physical Society and IOP Publishing Ltd

been settled. The estimation of the initial vectors of spatiotemporal chaotic signals becomes an important problem in many practical applications. Recently some useful results for estimating the initial vectors in terms of symbolic dynamics were reported.[14−22] In order to investigate the inverse problem of a complex spatiotemporal chaotic system, an approach was developed in Ref. [14] to recover the statistical characteristics of the initial vectors of the system with non-lattice coupling model. In Ref. [15] the authors further proposed an algorithm for estimating the statistical characteristics of the initial values of system using a time-varying mapping coefficient under the condition of weak coupling. However, all the above methods can recover only the statistical characteristics of the lattice initial sequences of the given CML system. The challenging problem is to develop a new algorithm for estimating the exact initial vectors of the CML model in many practical applications.[14−16] In Refs. [17]–[19], Wang *et al.* discussed the problem of recovering the initial vectors of a local CML system in terms of symbolic dynamics, which proved that each point in the CML system with Logistic mapping converges to the initial values of the CML with respect to sufficient backward iteration steps.[17] Based on the results in Ref. [17], the initial vectors of CML with both Logistic and Tent mapping functions are estimated. Moreover, the presented algorithm is extended to other CMLs with Piecewise Linear and Chebyshev mapping. However, the precondition of the above proposed algorithm is not always satisfied, and each point in state space cannot always converge to the initial value of the given CML. In fact, whether the initial value of the given CML can be recovered is directly determined by both coupling strength and mapping function.

According to the results of the initial vector estimation of a local CML in Refs. [21] and [22], in this paper we study the inverse problem of the global CML model and propose a novel computationally efficient algorithm for estimating the initial vectors of a global CML system in a wide range in terms of symbolic dynamics. It is theoretically proven that not all inverse chaotic mapping functions are satisfied for contraction mapping, but both Bernoulli and Tent inverse mappings are contracted. Moreover, the whole CD is developed to investigate the convergence condition of Logistic, Bernoulli and Tent mappings. It is found that the values in phase space do not always converge to their initial conditions with respect to sufficient backward iteration of the symbol vectors using the whole CD analysis. The CD and the coupling strength are relevant to the mapping function of the given CML model. The CD properties of Logistic, Bernoulli and Tent mapping functions are analysed and compared. The error bound for estimating the initial vector of globally CML is also presented to investigate the estimation errors with a wide range of coefficients. Several experimental results are provided to evaluate the estimation performance with different signal-to-noise ratios (SNRs), which confirms the proposed algorithm. This contribution has provided both theoretical and experimental results for studying and characterizing the spatiotemporal chaotic behaviours.

The rest of the present paper is organized as follows. In Section 2, a novel algorithm in terms of symbolic dynamics is proposed for estimating the initial vectors of the global CML system. In Section 3, the CD in backward iteration process of the inverse mapping is investigated for three kinds of CML models. In Section 4, the error bounds of the initial vector estimation with different SNRs are analysed to evaluate the performance of the global CML. Finally, Section 5 is devoted to the conclusions drawn from the present study.

2. Proposed method

A typical global CML model is described as[5]

$$x_{n+1}^i = (1-\varepsilon)f(x_n^i) + \frac{\varepsilon}{L}\sum_{j=1}^{L} f(x_n^j), \tag{1}$$

where $i = 1, 2, \ldots, L$ are the sequence numbers of model lattice sites, L represents the total lattice number, n denotes the number of iterative steps, and ε is the coupling coefficient with periodic boundary condition $\boldsymbol{x}(i+L) = \boldsymbol{x}(i)$. The mapping function $f : I \to I$ is the phase space. Let $\boldsymbol{P} = \{P_0, P_1, \ldots, P_{M-1}\}$ be a finite disjoint partition of a phase space I, i.e. $\bigcup_{j=0}^{j=M-1} P_j = I$ and $P_i \bigcap P_j = \phi (i \neq j)$. At time n, the symbolic vectors of the system can be defined as $\boldsymbol{s}_n = [s_n^1, s_n^2, \ldots, s_n^L]^{\mathrm{T}}$ so that the time series $\{\boldsymbol{s}_0, \boldsymbol{s}_1, \ldots, \boldsymbol{s}_n, \ldots\}$ is expressed as a symbol set of the given system.[13]

For Eq. (1), let $\boldsymbol{x}_n = [x_n^1, x_n^2, \ldots, x_n^L]^{\mathrm{T}}$, $\boldsymbol{f}(\boldsymbol{x}_n) = [f(x_n^1), f(x_n^2), \ldots, f(x_n^L)]^{\mathrm{T}}$, we have

$$\boldsymbol{x}_{n+1} = A \circ \boldsymbol{f}(\boldsymbol{x}_n), \tag{2}$$

where A is the coupling coefficient matrix given as

$$A=\begin{bmatrix} 1-\frac{L-1}{L}\varepsilon & \frac{\varepsilon}{L} & \frac{\varepsilon}{L} & \cdots & \frac{\varepsilon}{L} \\ \frac{\varepsilon}{L} & 1-\frac{L-1}{L}\varepsilon & \frac{\varepsilon}{L} & \cdots & \frac{\varepsilon}{L} \\ \vdots & \ddots & \ddots & \ddots & \vdots \\ \frac{\varepsilon}{L} & \frac{\varepsilon}{L} & \ddots & 1-\frac{L-1}{L}\varepsilon & \frac{\varepsilon}{L} \\ \frac{\varepsilon}{L} & \frac{\varepsilon}{L} & \cdots & \frac{\varepsilon}{L} & 1-\frac{L-1}{L}\varepsilon \end{bmatrix}_{L\times L}. \tag{3}$$

When $\varepsilon \neq 1$, we have $|A| \neq 0$ and A is reversible due to $|A| = (1-\varepsilon)^{L-1}$.

Based on Eq. (2), we have $\boldsymbol{f}(\boldsymbol{x}_n) = A^{-1}(\mathbf{x}_{n+1})$ and $\boldsymbol{x}_n = \boldsymbol{f}_{s_n}^{-1}(A^{-1}(\boldsymbol{x}_{n+1})) = \boldsymbol{f}_{s_n}^{-1} \circ A^{-1}(\boldsymbol{x}_{n+1})$. Let $\boldsymbol{H}_{s_n}^{-1} = \boldsymbol{f}_{s_n}^{-1} \circ A^{-1}$, the iterative algorithm for initial vector estimation of global CML can be given as

$$\boldsymbol{x}_n = \boldsymbol{f}_{s_n}^{-1} \circ A^{-1}(\boldsymbol{x}_{n+1}) = \boldsymbol{H}_{s_n}^{-1}(\boldsymbol{x}_{n+1}). \tag{4}$$

For the given $\boldsymbol{f}_{s_n}^{-1}$ and A^{-1}, accurate initial values can be obtained using Eq. (4), but we need to consider the CD of $\boldsymbol{H}_{s_n}^{-1}$. To discuss the CD of $\boldsymbol{H}_{s_n}^{-1}$, firstly the conception of contraction mapping theorem, whole convergence (WC) and whole divergence (WD) are discussed.

Lemma 1 Contraction mapping theorem

Let phase space (X, d) be complete metric space, map $G : X \to X$, for each $\boldsymbol{x}_n, \boldsymbol{y}_n \in X$, defines the distance measure

$$d(\boldsymbol{x}, \boldsymbol{y}) = \|\boldsymbol{x}_n - \boldsymbol{y}_n\| = \sum\nolimits_{i=1}^{L} \left|x_n^i - y_n^i\right|. \tag{5}$$

If γ exists such that $0 \leq \gamma < 1$, then we have $d(G\mathbf{x}_n, G\boldsymbol{y}_n) \leq \gamma d(\boldsymbol{x}_n, \boldsymbol{y}_n)$. Thus G is a contraction mapping on X. There exists a fixed point $\bar{x}$ for any initial value $x_0 \in X$, and we have $\lim_{n\to\infty} T^n x_0 = \bar{x}$. The γ_n is defined as the CD factor. When $0 < \gamma_n < 1$, γ_n is a convergent factor, and G is convergent at the n-th iteration step. Otherwise, γ_n is a divergent factor, while G is divergent at the n-th iteration step. If $0 < \gamma_n < 1$ for any n, G is a contraction mapping. Let $E = \{e_1, e_2, \ldots, e_I\}$, $Q = \{q_1, q_2, \ldots, q_J\}$, where $E \bigcup G = N$ and $E \bigcap G = \varphi$. If $n \in E, 0 < \gamma_n < 1$, and $n \in G$, $\gamma_n \geq 1$, G is convergent in some subsets of phase space X and divergent in other subsets. If the convergent strength is stronger than the divergent strength, the following relation is established:

$$\sum_{n=1}^{\infty} \gamma_n < \infty, \tag{6}$$

where G is regarded as WC. Otherwise, G becomes WD.

If $\boldsymbol{H}_{s_n}^{-1}$ is a contraction mapping, according to Eq. (4), we have

$$\hat{\boldsymbol{x}}(0|N) = \lim_{N\to\infty} \boldsymbol{H}_s^{-N}(\mu) = \boldsymbol{x}_0; \tag{7}$$

if $\boldsymbol{H}_{s_n}^{-1}$ is not a contraction mapping but WC, we have

$$\hat{\boldsymbol{x}}(0|N) = \lim_{N\to\infty} \boldsymbol{H}_s^{-N}(\mu) = \boldsymbol{x}_0 + \boldsymbol{\Psi}, \tag{8}$$

where $\boldsymbol{\Psi}$ denotes the estimation error.

In fact, the inverse mapping of a chaotic system and its topological conjugation are not always contraction mappings. In order to investigate the CD conditions and the corresponding theoretical basis, the whole CD of $\boldsymbol{H}_{s_n}^{-1}$ must be studied in detail.

3. The CD of inverse mapping $\boldsymbol{H}_{\boldsymbol{s_n}}^{-1}$

We firstly discuss the CD properties of A^{-1} and $\boldsymbol{f}_{\boldsymbol{s}_n}^{-1}$ so that the whole CD of $\boldsymbol{H}_{s_n}^{-1}$ can be provided.

3.1. The CD of inverse matrix $\boldsymbol{A^{-1}}$

For the coupling matrix A given in expression (3), let $A^{-1} = (a_{ij})_{L\times L}$ and define the norm of matrix $A^{-1} = (a_{ij})_{L\times L}$ as $\left\|A^{-1}\right\| = \max\limits_{1\leq j\leq L}(\sum\limits_{i=1}^{L}|a_{ij}|)$, then we will have

$$\begin{aligned} ||A^{-1}|| &= (1+\varepsilon)/(1-\varepsilon) - 2\varepsilon/[L(1-\varepsilon)] \\ &= [1+(1-2/L)\varepsilon]/(1-\varepsilon). \end{aligned} \tag{9}$$

Let $\boldsymbol{x}'_n = A^{-1}\boldsymbol{x}_n$, $\boldsymbol{y}'_n = A^{-1}\boldsymbol{y}_n$, and $||A|| = 1$ so that $\boldsymbol{x}_n = A\boldsymbol{x}'_n$ and $\boldsymbol{y}_n = A\boldsymbol{y}'_n$, and we will have

$$\begin{aligned} d(\boldsymbol{x}_n, \boldsymbol{y}_n) \leq d(\boldsymbol{x}'_n, \mathbf{y}'_n) &= \left\|A^{-1} \times \boldsymbol{x}_n - A^{-1} \times \boldsymbol{y}_n\right\| \\ &\leq \left\|A^{-1}\right\| d(\boldsymbol{x}_n, \boldsymbol{y}_n). \end{aligned} \tag{10}$$

Based on the contraction mapping Lemma, it can be seen from Eqs. (9) and (10) that A^{-1} is not a contraction mapping, but a divergence mapping.

Figure 1 shows the relationship of $||A^{-1}||$ with ε and L for $\varepsilon \in [0, 1)$. It can be seen that for a given

lattice size, $||A^{-1}||$ increases with coupling strength ε. When $\varepsilon \in [0, 0.5]$, $||A^{-1}||$ is almost kept unchanged with the increase of the coupling strength among the lattices. Moreover, the relation of $\|A^{-1}\| \geq 1$ is established for all given parameters.

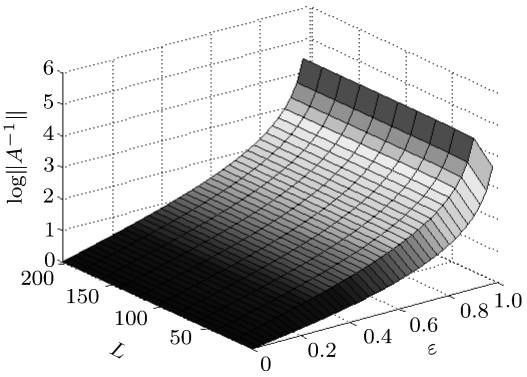


Fig. 1. Relationship of $||A^{-1}||$ with ε and L.

3.2. The CD property of inverse mapping

3.2.1. The CD property of $f_{Ls_n}^{-1}$ with Logistic mapping

For the Logistic mapping $f_L(x_n) = 1 - 2x_n^2$, the inverse mapping in phase space can be given as

$$\boldsymbol{f}_{Ls_n}^{-1}(\boldsymbol{x}_n) = (2\boldsymbol{s}_{n-1} - 1)\sqrt{(1 - \boldsymbol{x}_n)/2},$$

where

$$\boldsymbol{s}_{n-1} = \begin{cases} 0, & \boldsymbol{x}_{n-1} \in [-1, 0], \\ 1, & \boldsymbol{x}_{n-1} \in (0, 1]. \end{cases}$$

To discuss the CD property, we have

$$\begin{aligned} & d(\boldsymbol{f}_{Ls_n}^{-1}(\boldsymbol{x}_n), \boldsymbol{f}_{Ls_n}^{-1}(\boldsymbol{y}_n)) \\ & = \sum_{i=1}^{L} \left| \sqrt{(1 - x_n^i)/2} - \sqrt{(1 - y_n^i)/2} \right| \\ & \leq \max_{1 \leq i \leq L} \frac{\sqrt{2}}{2\left| \sqrt{1 - x_n^i} + \sqrt{1 - y_n^i} \right|} d(\boldsymbol{x}_n, \boldsymbol{y}_n). \end{aligned} \quad (11)$$

Let $k_{\boldsymbol{f}_{Ls_n}^{-1}}(n) = \max\limits_{1 \leq i \leq L} \left[\sqrt{2}/\left(2\left|\sqrt{1 - x_n^i} + \sqrt{1 - y_n^i}\right|\right)\right]$. We can discuss the CD property of $\boldsymbol{f}_L^{-1}$. Figure 2 shows the feature for analysing the Logistic mapping. It can be seen that the shadow area corresponds to $\Delta x \geq \Delta y$ and the white area corresponds to $\Delta x < \Delta y$. When $x \in (-0.25, 0.25)$, $\Delta x \geq \Delta y$, the divergence condition is satisfied for the inverse Logistic mapping. Figure 3 shows the CD property with the relation of $\sqrt{1 - x_n^q} + \sqrt{1 - y_n^q} = \sqrt{2}/2$. It can be seen that the white area corresponds to $\sqrt{1 - x_n^q} + \sqrt{1 - y_n^q} > \sqrt{2}/2$ and $k_{f_{Ls_n}^{-1}}(n) < 1$. From the definition of contraction mapping, the iteration of $\boldsymbol{f}_{Ls_n}^{-1}$ is convergent. However, the shadow area corresponds to the conditions of $\sqrt{1 - x_n^q} + \sqrt{1 - y_n^q} < \sqrt{2}/2$ and $k_{f_{Ls_n}^{-1}}(n) > 1$, the iteration of $\boldsymbol{f}_{Ls_n}^{-1}$ may be divergent or convergent.

It can be seen from Figs. 2 and 3 that most regions of the phase space of the inverse Logistic mapping are satisfied for convergence, whereas the divergence for some regions of the phase space still exists. The inverse Logistic mapping is not contraction mapping but wholly convergent. Thus for the given mapping function, it is necessary to discuss whether the inverse mapping is the contraction mapping so that the initial vectors of CML can be correctly recovered.

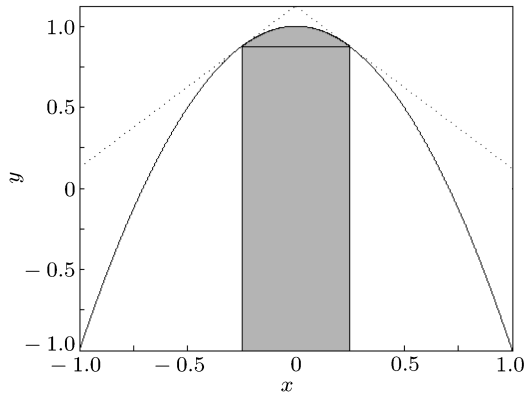


Fig. 2. Feature analysis of Logistic mapping (the shadow area for $\Delta x \geq \Delta y$ and the white area for $\Delta x < \Delta y$).

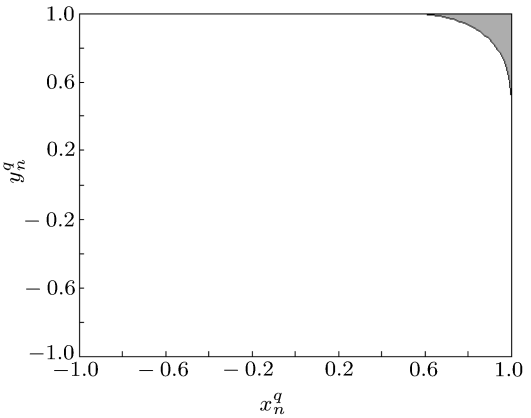


Fig. 3. Analysis of CD of Logistic inverse mapping.

3.2.2. The CD property of $f_{Bs_n}^{-1}$ with Bernoulli and Tent mappings

For Bernoulli mapping

$$f_B(x_n) = \begin{cases} 2x_n, & x_n \in [0, 0.5), \\ 2x_n - 1, & x_n \in [0.5, 1], \end{cases}$$

its inverse mapping in phase space can be defined as $\boldsymbol{f}^{-1}_{B\boldsymbol{s}_n}(\boldsymbol{x}_n) = (\boldsymbol{x}_n + \boldsymbol{b}_{n-1})/2$, where

$$\boldsymbol{b}_{n-1} = \begin{cases} 0, & \boldsymbol{x}_{n-1} \in [0, 0.5), \\ 1, & \boldsymbol{x}_{n-1} \in [0.5, 1]. \end{cases}$$

To investigate its CD property of $\boldsymbol{f}^{-1}_{Bs_n}$, we have the following expression:

$$\begin{aligned} d(\boldsymbol{f}^{-1}_{Bs_n}(\boldsymbol{x}_n), \boldsymbol{f}^{-1}_{Bs_n}(\boldsymbol{y}_n)) &= \sum_{i=1}^{L} \left| x_n^i - y_n^i \right| /2 \\ &= \|\boldsymbol{x}_n - \boldsymbol{y}_n\| /2 \\ &= 1/2 d(\boldsymbol{x}_n, \boldsymbol{y}_n). \end{aligned} \tag{12}$$

It can be seen that the CD factor of each iteration of Bernoulli mapping inverse system is 0.5, which shows that the mapping $\boldsymbol{f}^{-1}_{Bs_n}$ is globally contracted.

For the Tent mapping, based on the relationship of $H^{-1}_{\mu_n} = f^{-1}_{\mu_n} \circ A^{-1}$, it is assumed that divergence factor z of $H^{-1}_{s_n}$ represents $H^{-1}_{T\mu_n}$ which is the contraction mapping. In other words, we hope $f^{-1}_{\mu_n} \circ A^{-1} < 1$ and $f^{-1}_{\mu_n} = 1/2$, so that $z < 2$ can be established when $\|A^{-1}\| < 2$. If $\|A^{-1}\| \geq 2$, $H^{-1}_{T\mu_n}$ is convergent for $1 \leq z < 2$, but divergent for $2 \leq z \leq \|A^{-1}\|$.

Let the divergence factor z follow a normal distribution between 1 and $\|A^{-1}\|$, in which the mean value μ is $(\|A^{-1}\| + 1)/2$ and the variance is σ. The probability density function of z is given as

$$\Phi(z) = \begin{cases} \dfrac{1}{\sqrt{2\pi}\sigma} \exp\Big[-\dfrac{(z-\mu)^2}{2\sigma^2}\Big], & 1 \leq z \leq \left\|A^{-1}\right\|, \\ 0, & \text{otherwise.} \end{cases} \tag{13}$$

The divergence probability of $H^{-1}_{T\mu_n}$ can be estimated for $2 \leq z \leq \|A^{-1}\|$.

In addition, the convergence probability for one step iteration of $H^{-1}_{T\mu_n}$ can be given as

$$\phi(x) = \begin{cases} 1, & \|A^{-1}\| < 2, \\ \dfrac{\displaystyle\int_{x=1}^{2} \Big(\frac{1}{\sqrt{2\pi}\sigma} \exp\Big[-\frac{(x-\mu)^2}{2\sigma^2}\Big]\Big) \mathrm{d}x}{\displaystyle\int_{x=1}^{\|A^{-1}\|} \Big(\frac{1}{\sqrt{2\pi}\sigma} \exp\Big[-\frac{(x-\mu)^2}{2\sigma^2}\Big]\Big) \mathrm{d}x} \times 100\%, & \|A^{-1}\| \geq 2. \end{cases} \tag{14}$$

It can be seen from expression (14) that the convergence probability becomes small with the increase of $\|A^{-1}\|$ for $\|A^{-1}\| \geq 2$. When the iteration step of $H^{-1}_{T\mu_n}$ reaches N, the convergence probability is $\phi(z)^N$. Though A^{-1} mapping is divergent, Tent inverse mapping $f^{-1}_{s_n}$ is convergent. Thus, the CD of the inverse system $H^{-1}_{T\mu_n}$ is based on both A^{-1} and $f^{-1}_{s_n}$. When $\|A^{-1}\| < 2$, $H^{-1}_{T\mu_n}$ is absolutely convergent. On the other hand, $\|A^{-1}\|$ rapidly increases with coupling strength. $H^{-1}_{T\mu_n}$ becomes divergent. Obviously, the CD of $H^{-1}_{T\mu_n}$ is directly determined by A^{-1}. For example, when $\varepsilon \leq 0.25$ and $\|A^{-1}\| < 2$, the Tent mapping inverse system is the contraction mapping function.

3.3. The CD property of the whole inverse system

Based on the CD analyses of $\boldsymbol{f}^{-1}_{L\boldsymbol{s}_n}$ and A^{-1} with Logistic mapping, the CD of the whole inverse system $\boldsymbol{H}^{-1}_{L\boldsymbol{s}_n}$ can be systematically analysed. We have

$$\begin{aligned} &d(\boldsymbol{H}^{-1}_{Ls_n}(\boldsymbol{x}_n), \boldsymbol{H}^{-1}_{Ls_n}(\boldsymbol{y}_n)) \\ &\quad = d(\boldsymbol{f}^{-1}_{Ls_n}(\boldsymbol{x}'_n), \mathbf{f}^{-1}_{Ls_n}(\boldsymbol{y}'_n)) \\ &\quad = \sum_{i=1}^{L} \left| \sqrt{(1-\alpha_n^i)/2} - \sqrt{(1-\beta_n^i)/2} \right| \\ &\quad \leq \max_{1\leq i\leq L} \frac{\sqrt{2}}{2\left|\sqrt{1-\alpha_n^i} + \sqrt{1-\beta_n^i}\right|} d(\boldsymbol{x}'_n, \boldsymbol{y}'_n) \\ &\quad \leq \max_{1\leq i\leq L} \frac{\sqrt{2}}{2\left|\sqrt{1-\alpha_n^i} + \sqrt{1-\beta_n^i}\right|} \left\|A^{-1}\right\| d(\boldsymbol{x}_n, \boldsymbol{y}_n). \end{aligned} \tag{15}$$

When $\left\|A^{-1}\right\| = 1.0, 1.5, 2.0, 3.0$, the CD analysis of the whole inverse system $\boldsymbol{H}^{-1}_{L\boldsymbol{s}_n}$ is shown in Fig. 4, in which $\|A^{-1}\|$ fetch different values with the relation $\sqrt{1-\alpha_n^q} + \sqrt{1-\beta_n^q} = (\sqrt{2}\|A^{-1}\|/2)$. Based on the analyses of CD area and CD factors, it can be found that for the whole inverse iteration of the Logistic mapping, $\boldsymbol{H}^{-1}_{L\boldsymbol{s}_n}$ is wholly convergent, including the local divergence when convergence is absolutely dominant. The larger the $\|A^{-1}\|$, the smaller the possibility of convergence is.

Similarly, the CD of the whole inverse system with Bernoulli mapping can be obtained. Based on the CD analyses of $\boldsymbol{f}^{-1}_{B\boldsymbol{s}_n}$ and A^{-1} of Bernoulli mapping, for the CD of the whole inverse system $\boldsymbol{H}^{-1}_{B\boldsymbol{s}_n}$, we have

$$\begin{aligned} d(\boldsymbol{H}^{-1}_{Bs_n}(\boldsymbol{x}_n), \boldsymbol{H}^{-1}_{Bs_n}(\boldsymbol{y}_n)) &= d(\boldsymbol{f}^{-1}_{Bs_n}(\boldsymbol{x}'_n), \boldsymbol{f}^{-1}_{Bs_n}(\boldsymbol{y}'_n)) \\ &= 1/2 d(\boldsymbol{x}'_n, \boldsymbol{y}'_n) \\ &\leq 1/2 \left\|A^{-1}\right\| d(\boldsymbol{x}_n, \boldsymbol{y}_n). \end{aligned} \tag{16}$$

It can be seen that the CD of $\boldsymbol{H}^{-1}_{B\boldsymbol{s}_n}$ is determined by the sizes of both $\|A^{-1}\|$ and 0.5. According to inequality (10), we have $1/2d(\boldsymbol{x}_n, \boldsymbol{y}_n) \leq 1/2d(\boldsymbol{x}'_n, \boldsymbol{y}'_n) \leq 1/2\|A^{-1}\|d(\boldsymbol{x}_n, \boldsymbol{y}_n)$, which reveals that the range of CD factors of $\boldsymbol{H}^{-1}_{B\boldsymbol{s}_n}$ is between $[1/2, 1/2\|A^{-1}\|]$. When $\left\|A^{-1}\right\| < 2$, $\boldsymbol{H}^{-1}_{B\boldsymbol{s}_n}$ is contraction mapping, whereas $\boldsymbol{H}^{-1}_{B\boldsymbol{s}_n}$ is wholly convergent for $\|A^{-1}\| \geq 2$. If $\boldsymbol{H}^{-1}_{B\boldsymbol{s}_n}$ is contraction mapping or wholly convergent, the initial vectors of CML can be estimated to be

$$\begin{aligned}\boldsymbol{x}_n &= \boldsymbol{H}^{-1}_{Bs_n}(\boldsymbol{x}_{n+1}) = \boldsymbol{f}^{-1}_{Bs_n} \circ A^{-1}(\boldsymbol{x}_{n+1}) \\ &= [A^{-1}(\boldsymbol{x}_{n+1}) + \boldsymbol{b}_n]/2. \end{aligned} \tag{17}$$

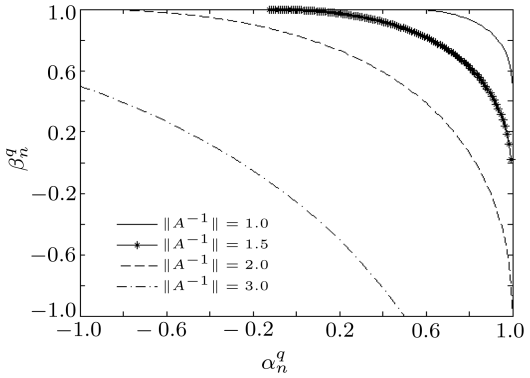


Fig. 4. The CD analysis of the whole inverse system.

4. Performance analysis

To analyse the estimation error, all CML initial values are randomly set to be in [0,1] or [−1,1] so that the universality of the algorithm can be tested. Then we collect each value x^i_n and symbolic dynamics s^i_n according to the inverse iteration of expression (4) to record the estimated value $\hat{x}^i_n$ at each iteration step. Finally, the estimation performances without noise and with a given SNR are investigated using MSE which is defined as:

$$\mathrm{MSE}(\hat{\boldsymbol{x}}_n) = 1/L \times \sum\nolimits_{i=1}^{L} (\hat{x}^i_n - x^i_n)^2.$$

First of all, the performance of initial value estimation without noise is evaluated. Both Logistic and Bernoulli mappings are used to analyse the performance of the global CML. The lattice size is set to be 20, and the iteration number is 20. Figure 5 shows the relationships between the iteration number and the

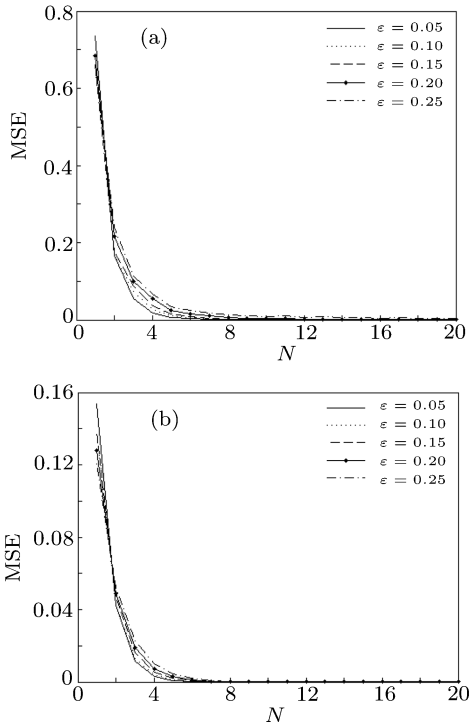


Fig. 5. The MSE analyses with different iteration steps for (a) Logistic mapping function and (b) Bernoulli mapping function.

initial value for $\varepsilon = 0.05, 0.10, 0.15, 0.20$, and 0.25, respectively. For weak coupling, when iteration number $N < 6$, the MSE of the estimation converges quickly to zero along iterative steps.

In Fig. 6, $\log_{10}$(MSE) is used to evaluate the performances with different iteration numbers and coupling strengths. For the Logistic mapping as shown in Fig. 6(a), the estimation error rapidly decreases with the increase of iteration number for small coupling strengths. However, divergence may happen when the coupling strength becomes larger. On the other hand, if the coupling strength is smaller than or equal to 0.34, the whole inverse system $\boldsymbol{H}^{-1}_{B\boldsymbol{s}_n}$ of Bernoulli mapping is contraction mapping. By comparing the estimation errors of Figs. 6(a) and 6(b), it can be seen that the convergence performance of $\boldsymbol{H}^{-1}_{B\boldsymbol{s}_n}$ is much better than that of $\boldsymbol{H}^{-1}_{L\boldsymbol{s}_n}$. In general, the performance of initial vector estimation is related to not only the coupling strength but also the mapping function.

Next, we study the performances of initial vector estimation with different SNRs. The chaotic signal with white Gaussian noise is given as

$$y^i_n = x^i_n + w^i_n, \quad i = 1, 2, \ldots, L;\ n = 1, 2, \ldots, N. \tag{18}$$

Figure 7 shows the simulation results of $\log_{10}$(MSE) changing with the iteration number and SNR for

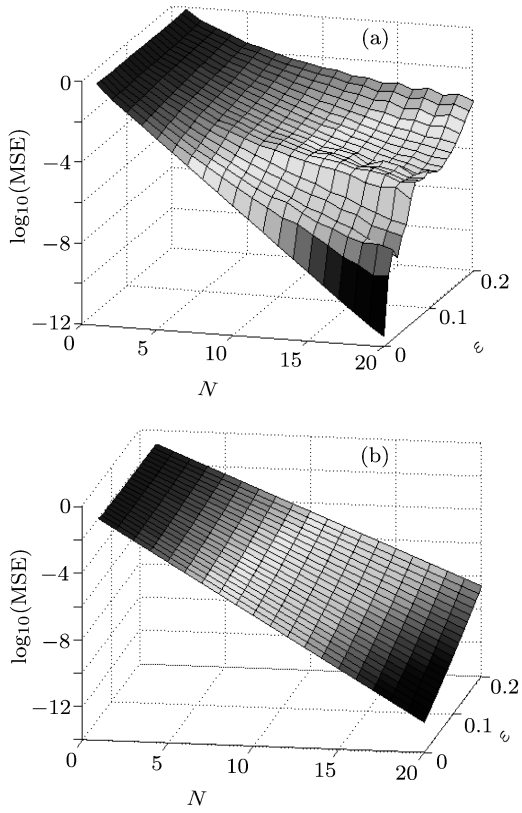


Fig. 6. Estimation error analyses with iteration number and coupling strength for (a) Logistic mapping and (b) Bernoulli mapping.

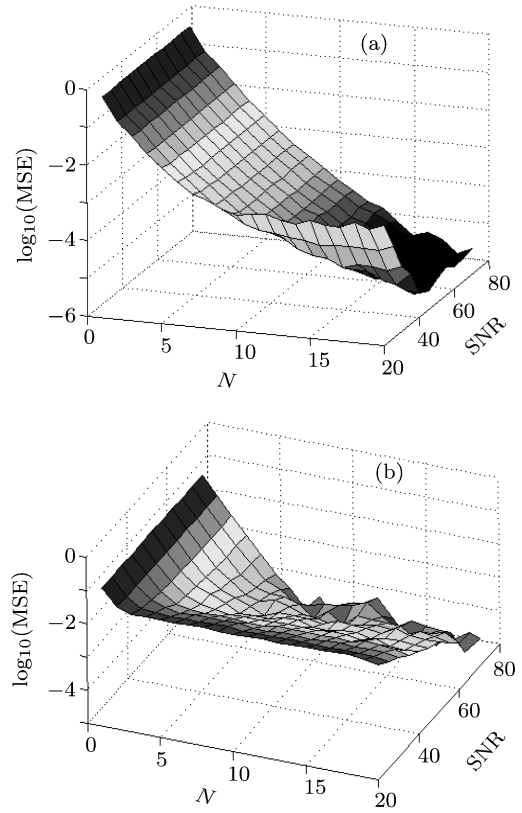


Fig. 7. Estimation errors changing with the iteration number and SNR for (a) Logistic mapping and (b) Bernoulli mapping.

Logistic and Bernoulli mappings. The coupling coefficient is set to be 0.1. It can be seen from the experimental results that the convergence performance is much better in the case of high SNR. However, for low SNR, the lower bound of $\log_{10}$(MSE) can only be reached with bigger iteration number as the added noise significantly affects the symbol estimation, which leads to the large $\log_{10}$(MSE). By comparing the results of Logistic and Bernoulli mappings, it can be found that the performance of Logistic mapping is generally better than that of Bernoulli mapping, which indicates that the initial vector estimation for Bernoulli mapping is sensitive to the added noise. It is proved that the CD performance using symbolic vector dynamics is significantly related to the given mapping function.

To further investigate the performances of the proposed algorithm with different SNRs, the Logistic mapping with 6 lattices is analysed to provide the experimental results. Figure 8 shows the corresponding results when SNR changes from 20 dB to 70 dB with iteration numbers being 10 and 20, and coupling strengths 0 and 0.01. Solid and dotted linear curves represent the Cramer–Rao lower bound (CRLB) of the error variance for iteration number $N = 10$ and 20, respectively. When the coupling strength is zero, the unbiased error variance progressively reaches the CRLB with increasing SNR, whereas the error variance progressively reaches the line parallel with CRLB for the coupling strength of 0.01 with increasing iteration number. For the same SNR, the estimated error is directly related to the coupling strength and iteration number. The estimation of the initial vectors becomes more accurate with smaller coupling strengths and bigger iteration number.

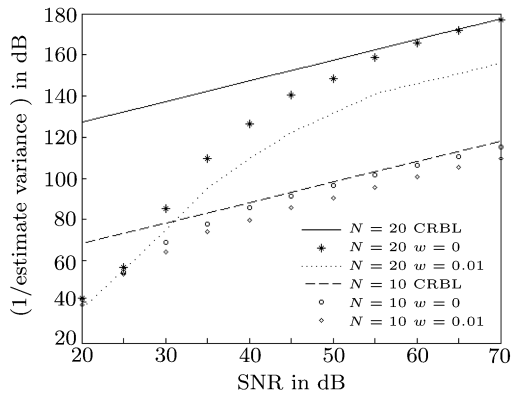


Fig. 8. The CRLB of the error variance for $N = 10$ and 20 with SNR varying from 20 dB to 70 dB.

5. Conclusions

A novel approach to the inverse problem of globally coupled map lattices is systematically investigated by utilizing symbolic vector dynamics. The relationship between the performance of initial condition estimation and the structural features of dynamical systems is theoretically analysed and proved. It is found that any point in a spatiotemporally coupled system does not necessarily converge to its initial value with respect to sufficient backward iteration, which is directly relevant to the coupling strength and mapping function. The CDs of Logistic, Bernoulli, and Tent mappings are analysed and compared. When the convergence is met, the error ranges in estimating the initial vector are investigated with different SNR conditions. Several simulations further confirm the proposed algorithm, and prove that the presented approach provides the important theoretical and experimental results for better analysing and characterizing the spatiotemporal complex behaviours in an actual system.

References

[1] Wang Y C, Zhao Q C and Wang A B 2008 *Chin. Phys.* B **17** 2373

[2] Shen M F, Ling L X, Chen J L and and Chang C Q 2010 *IEEE Trans. Inst. Meas.* **59** 1485

[3] Wang J L and Chen G Z 1999 *Acta Phys. Sin.* **48** 1605 (in Chinese)

[4] Wang H X and He C 2003 *Acta Phys. Sin.* **52** 2409 (in Chinese)

[5] Yang W M 1994 *Spatiotemporal Chaos and Coupled Map Lattice* (Shanghai: Shanghai Scientific and Technological Education Publishing House) p. 13 (in Chinese)

[6] Kaneko K 1989 *Physica* D **34** 1

[7] Kaneko K 1990 *Physica* D **41** 137

[8] Shinbrot T 1994 *Phys. Rev.* E **50** 3230

[9] Zheng W M and Hao B L 1994 *Applied Symbolic Dynamics* (Shanghai: Shanghai Scientific and Technological Education Publishing House) p. 50 (in Chinese)

[10] Xiao F H, Yan G R and Han Y H 2004 *Acta Phys. Sin.* **53** 2877 (in Chinese)

[11] Hao B L 1994 *Starting With Parabolas, An Introduction to Chaotic Dynamics* (Shanghai: Shanghai Scientific and Technological Education Publishing House) p. 20 (in Chinese)

[12] Buminovich L A 1997 *Physica* D*: Nonlinear Pheomena* **103** 1

[13] Shawn D P, Ned J C and Erik B 2006 *Phys. Rev. Lett.* **96** 034105

[14] Zeng Y C and Tong Q Y 2003 *Acta Phys. Sin.* **52** 285 (in Chinese)

[15] Liu Y, Shen M F and Chen H Y 2006 *Acta Phys. Sin.* **55** 564 (in Chinese)

[16] Pang Q, Wu W and Fan Y L 2007 *Acta Phys. Sin.* **56** 6836 (in Chinese)

[17] Wang K, Pei W J, Xia H S and He Z Y 2007 *Acta Phys. Sin.* **56** 3766 (in Chinese)

[18] Wang K, Pei W J, He Z Y and Cheung Y M 2007 *Phys. Lett.* A **367** 316

[19] Wang K, Pei W J, Wang S P, Cheung Y M and He Z Y 2008 *IEEE Trans. Ciruits Syst.* **55** 1116

[20] Shen M F, Liu Y and Lin L X 2009 *Chin. Phys.* B **18** 1761

[21] Shen M F, Lin L X, Li X Y and Chang C Q 2009 *Acta Phys. Sin.* **58** 2921 (in Chinese)

[22] Sun L S, Kang X Y and Lin L X 2010 *Chin. Phys.* B **19** 110507